JOURNAL OF VIROLOGY, Feb. 1997, p. 900–909 Vol. 71, No. 2
0022-538X/97/$04.00+0

Characterization of a Second Cleavage Site and Demonstration of Activity in *trans* by the Papain-Like Proteinase of the Murine Coronavirus Mouse Hepatitis Virus Strain A59

PEDRO J. BONILLA,† SCOTT A. HUGHES,‡ AND SUSAN R. WEISS*

Department of Microbiology, University of Pennsylvania, Philadelphia, Pennsylvania 19104-6076

Received 30 July 1996/Accepted 14 October 1996

The 21.7-kb replicase locus of mouse hepatitis virus strain A59 (MHV-A59) encodes several putative functional domains, including three proteinase domains. Encoded closest to the 5′ terminus of this locus is the first papain-like proteinase (PLP-1) (S. C. Baker et al., J. Virol. 67:6056–6063, 1993; H.-J. Lee et al., Virology 180:567–582, 1991). This cysteine proteinase is responsible for the in vitro cleavage of p28, a polypeptide that is also present in MHV-A59-infected cells. Cleavage at a second site was recently reported for this proteinase (P. J. Bonilla et al., Virology 209:489–497, 1995). This new cleavage site maps to the same region as the predicted site of the C terminus of p65, a viral polypeptide detected in infected cells. In this study, microsequencing analysis of the radiolabeled downstream cleavage product and deletion mutagenesis analysis were used to identify the scissile bond of the second cleavage site to between Ala832 and Gly833. The effects of mutations between the P5 and P2′ positions on the processing at the second cleavage site were analyzed. Most substitutions at the P4, P3, P2, and P2′ positions were permissive for cleavage. With the exceptions of a conservative P1 mutation, Ala832Gly, and a conservative P5 mutation, Arg828Lys, substitutions at the P5, P1, and P1′ positions severely diminished second-site proteolysis. Mutants in which the p28 cleavage site (Gly247 ↓ Val248) was replaced by the Ala832 ↓ Gly833 cleavage site and vice versa were found to retain processing activity. Contrary to previous reports, we determined that the PLP-1 has the ability to process in *trans* at either the p28 site or both cleavage sites, depending on the choice of substrate. The results from this study suggest a greater role by the PLP-1 in the processing of the replicase locus in vivo.

The murine coronavirus mouse hepatitis virus A59 (MHV-A59) has a single-stranded genome of positive polarity that is 31.3 kb long. Located at the 5′ end of the genome is the 21.7-kb-long gene 1, the putative replicase locus (4, 26). This locus is organized in two overlapping open reading frames (ORFs), ORF1a and ORF1b. These ORFs are predicted to encode several functional domains (4, 7, 16, 17, 19, 26). Depending on the coronavirus species, ORF1a contains one or two cysteine proteinase domains distantly related to the cellular proteinase papain. MHV-A59 has two of these papain-like proteinase domains, but only the one encoded closest to the 5′ end of the viral genome, the PLP-1, has been characterized (3, 5). In vitro studies of this proteinase have identified its core domain and catalytic Cys1121 and His1272 residues (3, 5). In cell-free expression experiments, the PLP-1 cleaves between ORF1a amino acids Gly247 and Val248 to generate the amino-terminal polypeptide p28 (14, 20). Found immediately downstream of the PLP-1 is a motif of unknown function conserved among several viral families designated the X domain (18). Downstream of the PLP-1 and X domains is the second putative papain-like proteinase of MHV, for which no enzymatic activity has yet been demonstrated. All of the coronavirus replicase loci studied so far encode a poliovirus 3C-like proteinase; activity for this domain was recently demonstrated in three different coronaviruses, including MHV-A59 (27–29, 36). A predicted growth hormone-like domain is near the 3′ end of ORF1a. Putative polymerase, helicase, and zinc finger motifs are found within ORF1b.

In MHV-A59, ORF1a and ORF1b potentially encode two very large polypeptides of 496 and 309 kDa, respectively. Translation of these ORFs via a frameshift mechanism would result in the expression of a polyprotein of more than 800 kDa. Some or all of the three ORF1a-encoded proteinases are believed to process the replicase polyprotein into mature polypeptides. Some of the ORF1a-encoded proteins expressed intracellularly have been identified (12, 13, 23, 34). The first virus-encoded nonstructural polypeptide identified was the N-terminal p28, which is rapidly processed from the ORF1a polyprotein. Because p28 is processed in vitro by the PLP-1, it is believed that the same proteinase is responsible for its processing in vivo. Experimental evidence indicates that the polypeptide encoded immediately downstream of p28 is p65 (13). The processing of this polypeptide has slower kinetics compared to p28 in infected cells. It is further believed that the next adjacent product is p290 and that it encompasses the PLP-1. This polypeptide is further processed into p50 polypeptide (which includes the PLP-1) and p240 (12). Together, these polypeptides may account for approximately 77% of the ORF1a coding region. In addition, some ORF1b-specific polypeptides have been identified (11). Except for the enzymatic functions of the PLP-1 and the 3C-like proteinase and the zinc-binding capacity of a cysteine-rich domain of ORF 1b (29a, 35), the roles of these viral polypeptides remain to be determined.

During in vitro translation of MHV-A59 genomic RNA or synthetic RNA from plasmids containing the N-terminal 5.4 kb of ORF1a, only proteolytic products resulting from cleavage at the p28 site are observed (3, 5). However, we recently reported a second PLP-1 cleavage activity, in addition to the in vitro

* Corresponding author. E-mail: weisssr@mail.med.upenn.edu.
† Present address: Division of Molecular Virology, Baylor College of Medicine, Houston, TX 77030.
‡ Present address: Institut de Recherches Cliniques de Montreal, Montreal PQ H2W-1R7, Canada.

TABLE 1. Primers used for PCR amplifications and mutagenesis

Name	Nucleotide sequence[a] (5′-3′)	ORF1a position
FSP 2013-2036	AGCCATGAGGTGACTGACATGTGT	2013–2036
RSP 2828-2805	CTCTGAACACGCCTTCGAAAGAAC	2828–2805[b]
Deletion mutagenesis primers		
FMP ΔMsc.2	GATGTTAAAGTGGCC|AACGACACTGTTGGCGTGTTA	2064–2078, 2658–2678
FMP ΔMsc.3	GATGTTAAAGTGGCCACT|CAGTGCTGGAGGTTTCCCT	2064–2081, 2682–2700
FMP ΔMsc.4	AAAGTGGCC|AAAGTCGAGTTTAACGACAAGCCC	2070–2078, 2712–2735
FMP ΔAG	AGTGCTGGAGGTTTCCCTGT|AAGAAAGTCGAGTTTAACGAC	2683–2702, 2709–2729
FMP ΔAK	GAAGAGGACGGCGTT|GGGCAGGTTGAGG	3138–3152, 3159–3171
FMP ΔGD	CTTGCAAATTCGCCACCTGT|GGTCTTGTACCCCTCCTAC	1894–1913, 1920–1938
P5-P2′ mutagenesis primers		
FMP K834R,T	GTTTCCCTGTGCGGGCA(G,C)GAAAGTCGAGTTTAACG	2693–2727
FMP G833A,V	TTCCCTGTGCGG(C,T)CAAGAAAGTCGA	2695–2719
FMP G833D	GTTTCCCTGTGCGG(A)CAAGAAAGTCGAG	2693–2720
FMP A832G,E,V	GGTTTCCCTGTG(G,A,T)GGGCAAGAAAGT	2692–2716
FMP C831G,R,S	CTGGAGGTTTCCC(G,C,A)GTGCGGGCAAGAAAG	2687–2715
FMP P830A,S,T	GCTGGAGGTTT(G,T,A)CCTGTGCGGGCAAGAAAG	2686–2715
FMP F829C,S,Y	CAGTGCTGGAGGT(G,C,A)TCCCTGTGCGG	2682–2706
FMP R828M,T	GATCAGTGCTGGA(T,C)GTTTCCCTGTGCG	2679–2714
FMP R828K	GATCAGTGCTGGA(A)GTTTCCCTGTGC	2679–2713
FMP R828M,C831R	CTGGA(T)GTTTCCC(C)GTGCGGGCAAGAAAG	2687–2715
Cleavage site exchange mutagenesis primers		
FMP RGV→RAG	GGCTATCGCG(C)TG(G)TAAGCCCATC	939–962
FMP CAG→RGV	GGAGGTTTCCC(C)GTG(G)GG(T)CAAGAAAGTCGAG	2689–2720

[a] A vertical line within the primer sequence indicates noncontiguous sequences in the viral genome. Mutant nucleotides are shown in parentheses. Degenerate primers at one position are indicated by the presence of more than one nucleotide in parentheses.
[b] Reversed order of ORF1a position numbers indicates a negative-strand primer.

processing of p28 (5). The translation products of some plasmids containing a partial deletion of the coding region between p28 and the PLP-1 indicated the presence of a second cleavage site downstream of the p28 site. To further our understanding of the MHV-A59 PLP-1 and its role on the processing of the coronavirus replicase locus, we studied this new cleavage site. Deletion analysis was used to map the location of the second cleavage site to a short stretch of amino acids. The location of the scissile bond, between Ala832 and Gly833, was deduced after N-terminal sequencing of the p90 radiolabeled cleavage product and deletion mutagenesis analysis. This cleavage site resembles a typical viral papain-like cleavage site. Interestingly, this second cleavage site corresponds in position to the expected cleavage site that would produce the C terminus of p65, a product observed in MHV-A59-infected cells (13). We analyzed the role that amino acids near the cleavage site play in proteolytic processing. The PLP-1 is able to process the p28 cleavage sequence at the second position as well as the second-site sequence at the p28 site. Here we also first report that like a number of other viral proteinases, the PLP-1 has the ability to process substrates in *trans*. Thus, the newly described in vitro activities of the PLP-1 suggest a more extensive role for this proteinase in vivo.

MATERIALS AND METHODS

Plasmids. The MHV-A59 ORF1a expression vectors pSPNK, ΔMsc, ΔMBst, and ΔMsc H1272R have been described elsewhere (5). pSPNK encodes the first 1,484 amino acids of gene 1 ORF1a. Like pSPNK, ΔMsc and ΔMBst extend to ORF1a amino acid 1484 but have in-frame deletions of 181 (between Ala623 and Lys805) and 245 (between Ala623 and Lys869) amino acids, respectively. ΔMsc H1272R is identical to ΔMsc except for the substitution of the catalytic His1272 with an arginine. This mutation inactivates PLP-1 activity (5). The pSPNK RGV→RGG and RGV→RAV p28 cleavage site mutants have been described elsewhere (20). The deletion in ΔMsc was progressively extended by PCR mutagenesis. Mutagenesis primers FMP ΔMsc.2, FMP ΔMsc.3, and FMP ΔMsc.4 (Table 1) were used in combination with RSP 2828-2805 to generate the new deletion constructs ΔMsc.2, ΔMsc.3, and ΔMsc.4, respectively. PCR amplifications were performed by using ΔMsc as the template and Vent DNA polymerase as previously described (5). After purification, the amplification products were cut with restriction enzymes *Msc*I and *Bst*BI. These fragments were cloned into the corresponding sites in ΔMsc. The deletions in ΔMsc.2, ΔMsc.3, and ΔMsc.4 extend between MHV-A59 ORF1a amino acids Ala623 to Asn817, Thr624 to Gln825, and Ala623 to Lys835, respectively (Fig. 1A). To generate ΔAG, a first round of PCR was performed with primers FMP ΔAG and RSP 2828-2805. The amplification product of this first PCR amplification was then used as a megaprimer for a second round of PCR in combination with primers FSP 2013-2036 and RSP 2828-2805. This second PCR product was then cloned into ΔMsc. ΔAG is similar to ΔMsc except for the additional in-frame deletion of the ORF1a Ala832 and Gly833 codons. Two other in-frame deletion mutants, ΔGD and ΔAK, were prepared by using the MORPH system (see below). ΔGD and ΔAK are also derived from ΔMsc and resemble ΔAG but instead have in-frame deletions of the 569-GlyAsp-570 and 982-AlaLys-983 ORF1a codons, respectively, in addition to the deletion present in ΔMsc. Single, double, and triple substitutions between amino acids 828 and 834 were performed by using the MORPH site-specific plasmid DNA mutagenesis kit (5 Prime-3 Prime, Inc.) as recommended by the manufacturer. The presence of the desired mutations and deletions was confirmed by DNA sequence analysis.

In vitro transcription and translations. Plasmid DNAs were expressed by using the TnT rabbit reticulocyte lysate coupled transcription-translation system (Promega) as previously described (5) with the exception of PLP-1 enzyme translations for *trans*-cleavage assays, in which [^{35}S]methionine was substituted with 1 mM methionine. The incorporation of [^{35}S]methionine into acid-precipitable counts was used as an indicator of protein synthesis. Lysate volumes containing equivalent amounts of acid-precipitable counts were directly analyzed by sodium dodecyl sulfate (SDS)-polyacrylamide gel electrophoresis (PAGE) or immunoprecipitated with polyclonal antisera as described before (11). The antisera used in this study have been described elsewhere (5). Immunoprecipitated products were analyzed on SDS-polyacrylamide gels. After electrophoresis, gels were treated with Autofluor (National Diagnostics), dried at 80°C under vacuum, and exposed to X-ray films at −80°C.

Radiosequencing of the N terminus of p90. The p90 downstream cleavage product was isolated to determine the sequence of the new in vitro cleavage site. Microsequencing of the p90 N terminus was done as previously described, with the following modifications (20). In vitro transcription-translation of ΔMsc was performed in the presence of 250 μCi of [^{3}H]valine (NEN/DuPont). The translation products were electrophoresed and then transferred onto a polyvinylidene difluoride membrane (Bio-Rad). Next, the position of the band corresponding to

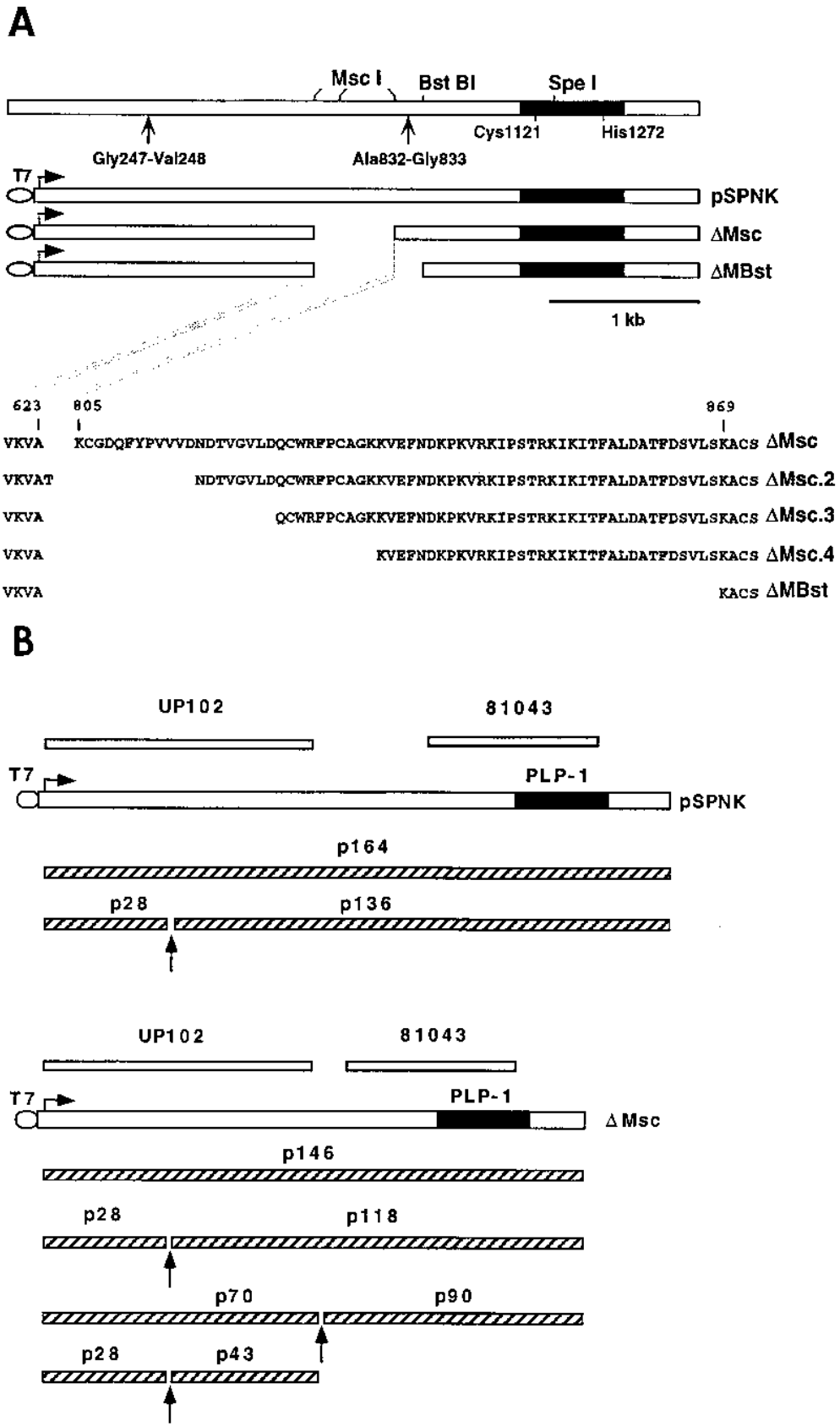

FIG. 1. Partial map of the murine coronavirus ORF1a: diagrams of plasmid DNAs and polypeptides that they encode. (A) The first 4.7 kb of ORF1a, including the leader papain-like proteinase, or PLP-1 (black boxes). The positions of the amino acids that comprise the catalytic dyad, Cys1121 and His1272, are indicated. The arrows indicate the locations of the p28 cleavage site (Arg247 ↓ Gly248) and second cleavage site (Ala832 ↓ Gly833). All plasmids are under the transcriptional control of the T7 promoter. The rightward arrow above each plasmid diagram indicates the translation initiation site. Details of the amino acid deletions in ΔMsc, ΔMsc.2, ΔMsc.3, ΔMsc.4, and ΔMBst are shown below. The parental construct ΔMsc has a deletion of 181 amino acids between Ala623 and Lys805. (B) The plasmid constructs are depicted as in panel A. The polypeptides synthesized after in vitro transcription-translation are shown below each plasmid diagram. The regions encoding the epitopes recognized by the polyclonal antisera UP102 and 81043 are shown above (shaded boxes).

TABLE 2. Viral papain-like proteinase cleavage sites

Virus[a]	Proteinase (cleavage site)[b]	Amino acid sequence[c]							Reference(s)
		P5	P4	P3	P2	P1 ↓ P1′		P2′	
BBScV[d]	p223 (helicase ↓ polymerase)	K	N	L	L	G	A	D	25
BYV[d]	N terminus of ORF1a	P	R	F	I	G	G	V	1
CB HAV	p29 (p29 ↓ p40)	L	A	R	I	G	G	R	10
	p48	D	I	L	V	G	A	E	30
EAV	nsP1 (nsP1 ↓ nsP2)	A	G	N	Y	G	G	Y	31
FMDV	Lb pro (eIF-4γ)[e]	F	A	N	L	G	R	P	24
	Lb pro (L ↓ VP4)	Q	R	K	L	K	G	A	24
MHV	PLP-1 (p28 ↓ p65)	K,R	G	Y	R	G	V	K	14, 20
	PLP-1 (Ala832 ↓ Gly833)	R	F	P	C	A	G	K	This study
RUB	P200 (P150 ↓ P90)	L	S	R	G	G	G	T	9
Alphaviruses	nsP2 (nsP1 ↓ nsP2)	X	X	A,I	G	A	A,G	X	32
	nsP2 (nsP2 ↓ nsP3)	X	X	A,V,S	G	C,A,R	A	P	32
	nsP2 (nsP3 ↓ nsP4)	X	X	A,V	G	A,G	Y	I	32
TEV	HC-Pro	T	Y	N	V	G	G	M	8
TYMV	p206 (p150 ↓ p70)	K	L	N	G	A	T	P	6, 21

[a] Abbreviations: BBScV, blueberry scorch virus; BYV, beet yellows closterovirus; CB HAV, chestnut blight hypovirulence-associated virus; EAV, equine arteritis virus; FMDV, foot-and-mouth disease virus; MHV, mouse hepatitis virus; RUB, rubella virus; TEV, tobacco etch virus; TYMV, turnip yellow mosaic virus.

[b] The cleavage target or cleavage site is shown in parentheses.

[c] Cleavage occurs between the P1 and P1′ amino acids, as indicated by the arrow. In the consensus data presented for the nsP2 cleavage sites of several alphaviruses, the X represents any amino acid (32).

[d] Preliminary identification based on computer-assisted sequence analysis and cleavage inhibition by site-directed mutagenesis of the residue at the P1 position (Gly1472 for BBScV and Gly588 for BYV).

[e] The eIF-4γ substrate is a cellular protein involved in the translation of mRNAs.

the p90 C-terminal cleavage product was identified by autoradiography, and 100 mm^2 of membrane to which p90 was immobilized was subjected to Edman degradation. Eluate collected from each cycle of Edman degradation was added to scintillation cocktail (ICN) and counted in a liquid scintillation counter (Beckman).

Quantitative analysis of p90 and p136 cleavage. Plasmid ΔMsc produces a 146-kDa polypeptide (p146) that is proteolytically cleaved by the PLP-1 at two sites. Complete processing of p146 produces the N-terminal cleavage product (p28), a 43-kDa polypeptide downstream from p28 (p43), and the C-terminal polypeptide (p90). The C-terminal polypeptide has a predicted mass of 71 kDa but exhibits a slow migration on SDS-polyacrylamide gels, thus the p90 designation. In addition, partial processing at only the p28 site produces p118, the full-length precursor without p28. Similarly, cleavage only at the second site produces p70 (p70 = p28 + p43) in addition to p90. The processing of the p90 cleavage product was analyzed by using a Molecular Dynamics PhosphorImager 445 SI as described before (5), with the following modifications. Equivalent amounts of acid-precipitable counts from the translations of each construct were used for electrophoresis on SDS–9% polyacrylamide gels. Gels were processed, dried, and exposed to a storage phosphor screen overnight. For each plasmid, the intensity of p146 and each cleavage product was determined from the collected images. The in vitro p90 cleavage activity of each construct was calculated as the ratio of p90 intensity versus the total amount of protein: p90/(p146 + p118 + p90 + p70 + p43 + p28). The activity of each mutant was then compared to that of ΔMsc to determine a relative percentage of cleavage activity. Mutants were classified into four groups of normalized percentage of activity: ++, +, −/+, and −, corresponding to 81 to 100%, 41 to 80%, 21 to 40%, and less than 20% of the activity of ΔMsc. For pSPNK and site-directed mutants derived from pSPNK, processing of the p136 cleavage product was analyzed as described before (20).

Posttranslational *trans* cleavage assays. PLP-1 enzyme was synthesized from pSPNK or ΔMsc template in the absence of a radioactively labeled amino acid (see above). Substrates were derived from either pSPNK H1272P or ΔMsc H1272R, linearized with *Spe*I, and translated in the presence of [^{35}S]methionine. The *Spe*I-truncated templates produce polypeptides that extend to the ORF1a amino acid Lys1162. These truncated polypeptides lack the C terminus of the PLP-1 which contains the catalytic His1272 and are proteolytically inactive. Coupled in vitro transcription-translation reaction mixtures were incubated at 30°C for 1 h. After addition of 1/10 volume of stop buffer (0.6 U of RQ DNase I per μl, 1.6 μg of RNase A per μl, 20 mM methionine) to each reaction, samples were further incubated at 30°C for 15 min. Equal volumes of [^{35}S]methionine-labeled substrate and unlabeled enzyme were mixed. The different enzyme and substrate combinations tested are indicated in Fig. 6. Samples were further incubated at 20°C for 14 to 16 h. Either 1× volumes of the enzyme-only and substrate-only reactions or 2× volumes of the enzyme-substrate mix reactions were used for electrophoretic analysis. To confirm the absence of protein synthesis after the addition of stop buffer, 0.5 μl of [^{35}S]methionine (10 μCi/μl) was added to a portion of each unlabeled enzyme reaction. As expected, none of these control reactions generated detectable radiolabeled polypeptides (data not shown) due to the degradation of the DNA and RNA templates by the added nucleases and the presence of excess unlabeled methionine.

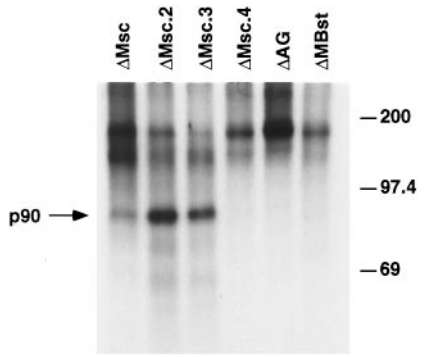

FIG. 2. Mapping of the second cleavage site by deletion analysis. Plasmid DNAs were in vitro transcribed and translated in TnT rabbit reticulocyte lysate in the presence of [^{35}S]methionine as described in Materials and Methods. Equivalent amounts of acid-precipitable counts from each lysate were immunoprecipitated with the polyclonal antiserum 81043. Immunoprecipitated products were analyzed by SDS-PAGE (10% gel). The specific plasmid used in each reaction is indicated above each lane. The arrow to the left indicates the migration of the C-terminal cleavage product p90. The molecular masses of ^{14}C-labeled protein markers are indicated in kilodaltons to the right.

RESULTS

Deletion mapping of the second in vitro cleavage site. The murine coronavirus PLP-1 is responsible for the in vitro cleavage of p28. This has been demonstrated after in vitro translation of mRNAs derived from the first 4.7 kb of the coronavirus genome (2, 3, 5, 20). We previously reported that in vitro expression of the MHV-A59 deletion construct ΔMsc produces a second PLP-1-mediated cleavage event, downstream from where the p28 cleavage occurs (5). The translation products of ΔMsc include p43, p70, and p90 in addition to p28 (Fig. 1B). However, expression of ΔMBst, a plasmid similar to ΔMsc except for a further extension of the ORF1a deletion by 64 amino acids, produces only p28 and none of the cleavage

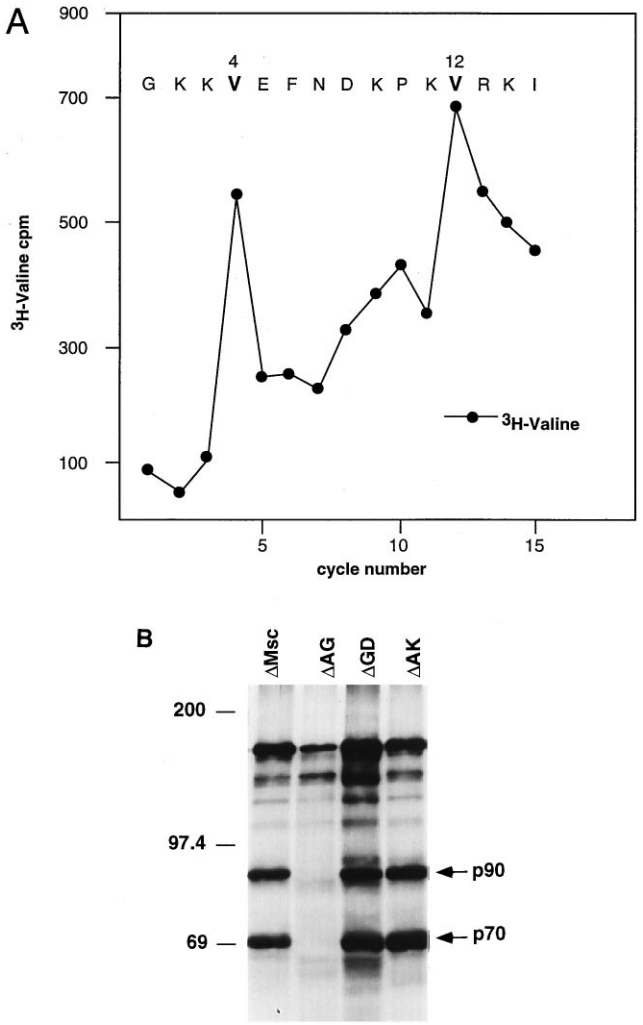

FIG. 3. Determination of the second cleavage site. (A) Microsequence analysis of the N terminus of [^{3}H]valine-labeled p90 cleavage product. The p90 cleavage product was generated by coupled in vitro transcription-translation of ΔMsc in the presence of [^{3}H]valine. The cleavage product was resolved by SDS-PAGE, transferred onto a polyvinylidene difluoride membrane, and subjected to Edman degradation. The amino acid fraction from each cycle was analyzed by scintillation counting. The plot shows the total counts per minute of each fraction along the *y* axis and the Edman degradation cycle along the *x* axis. The amino acid sequence shown was deduced from the positions of the radioactivity peaks and other data (see text). (B) SDS-PAGE analysis of radiolabeled translation products from ΔMsc, ΔAG, ΔGD, and ΔAK. Plasmid DNA was in vitro transcribed and translated in TnT rabbit reticulocyte lysate in the presence of [^{35}S]methionine as described in Materials and Methods. Volumes of the radiolabeled lysates containing equivalent amounts of acid-precipitable counts were analyzed by SDS-PAGE (9% gel). The specific plasmid used in each reaction is indicated above each lane. The arrows to the right indicate the migration of the second-site cleavage products p90 and p70. The molecular masses of ^{14}C-labeled protein markers are indicated in kilodaltons to the left.

products derived from processing at this second site. Presumably the second cleavage site is absent from ΔMBst and located within this 64-amino-acid region of ORF1a between Lys805 and Ser868.

To better understand the processing of the MHV-A59 polyprotein by the PLP-1, we further studied this second cleavage event. We examined the 64-amino-acid region for the presence of a potential viral papain-like proteinase cleavage site, which usually occurs between amino acids with small uncharged side chains (Table 2). Usually a glycine or an alanine is found at the P1 position. Although a wider array of amino acids can be found at the P1′ position, there is a marked preference for glycine or alanine. An alanine-glycine dipeptide corresponding to ORF 1a amino acids 832 and 833 was identified as a potential cleavage site. Processing at this site in ΔMsc would result in the production of cleavage products in close agreement with those observed after in vitro translation. Moreover, proteolytic processing at the p28 cleavage site and this site in vivo would generate a 64.8-kDa polypeptide that is similar in mass to the p65 polypeptide observed in infected cells. This potential cleavage site is conserved in the JHM and A59 strains of MHV (4, 26).

To study the relationship between the 832-AlaGly-833 dipeptide and the second cleavage site, the deletion in ΔMsc was progressively extended (Fig. 1A). The 832-AlaGly-833 dipeptide is present in the deletion plasmids ΔMsc.2 and ΔMsc.3 but absent from ΔMsc.4 (Fig. 1A). The [^{35}S]methionine-labeled translation products generated from these deletion constructs were immunoprecipitated with polyclonal antiserum 81043. This antiserum recognizes ORF1a epitopes present between ORF1a amino acids 871 and 1322, a region that includes most of the PLP-1 domain (Fig. 1B). The immunoprecipitation products were analyzed by SDS-PAGE (Fig. 2). Because p90 is a second-site-specific cleavage product, the presence of p90 after 81043 immunoprecipitation serves as an indicator of second cleavage site activity in these constructs. The p90 cleavage product was immunoprecipitated from the translation reaction of ΔMsc. Two other polypeptides of slower migration, immunoprecipitated also with 81043, correspond to the full-length translation product of ΔMsc (p146) and the full-length-minus-p28 cleavage product (p118). As previously observed, no p90 was immunoprecipitated from the translation of ΔMBst. The p90 cleavage product was immunoprecipitated from the translation reactions of ΔMsc.2 and ΔMsc.3 but not ΔMsc.4. ΔMsc.4 differs from ΔMsc.3 by only 10 amino acids, which include the potential cleavage site dipeptide 832-AlaGly-833. To further investigate the relationship between this dipeptide and the second cleavage, a double-deletion mutant was prepared. This mutant, ΔAG, is identical to the parental ΔMsc except for the additional in-frame deletion of the Ala832 and Gly833 codons. No p90 was immunoprecipitated from the translation reaction of ΔAG. These results suggest that the second cleavage site is within a short stretch of amino acids between Gln825 and Lys834. The absence of cleavage at the second site in ΔAG also suggests that the scissile bond may be between or adjacent to one of these two amino acids.

Radiosequence analysis of the [^{3}H]valine labeled p90 cleavage product. Inspection of the sequence downstream of the putative Ala832 ↓ Gly833 cleavage site indicated that sequencing of [^{3}H]lysine-labeled and [^{3}H]valine-labeled p90 would unambiguously identify the cleavage site. However, we were unable to incorporate enough [^{3}H]lysine into the p90 cleavage product for N-terminal sequencing. The results of the radiosequencing of the [^{3}H]valine-labeled p90 are shown in Fig. 3A. Radioactivity peaks were observed for fractions 4 and 12 obtained after Edman degradation of the radiolabeled p90. The ORF1a amino acid sequence encoded by ΔMsc was examined for the presence of the amino acid pattern X_3VX_7V, where X represents any amino acid except valine. Three sequences consistent with this pattern are encoded by ΔMsc: 570-DGLVP LLLDGLV-581, 833-GKKVEFNDKPKV-844, and 983-KG QVEADSEICV-994. The second of these three sequences contains Gly833 at the amino end and is compatible with the results of the deletion mapping, implicating the 832-AlaGly-833 dipeptide as the cleavage site (see above). With charged residues at the putative P1′ position, the other two sequences

Arg828 P5	Phe829 P4	Pro830 P3	Cys831 P2	Ala832 P1	Gly833 P1'	Lys834 P2'
Lys (++)	Cys (++)	Ala (+)	Arg (++)*	Glu (-/+)	Ala (-/+)	Arg (++)*
Met (-/+)	Ser (+)	Ser (-/+)	Gly (-)	Gly (++)*	Asp (-/+)	Thr (++)*
Thr (-)	Tyr (++)*	Thr (+)	Ser (++)	Val (-/+)	Val (-)	
Met			Arg (+)			
			Arg	Gly	Val (+)	

FIG. 4. Activities of amino acid substitutions near the Ala832 ↓ Gly833 cleavage site. The MHV-A59 ORF1a amino acid sequence from residues 828 to 834, corresponding to cleavage site positions P5 to P2′, respectively, is shown at the top. The cleavage site is between Ala823 (P1) and Gly833 (P1′). Individual mutations introduced into the ΔMsc plasmid between the P5 and P2′ positions are shown below. PhosphorImager analysis was used to classify each mutant into one of four activity groups as indicated in parentheses. The pair of boxed amino acids corresponds to an Arg828Met-Cys831Arg double mutant. The trio of boxed amino acids corresponds to a Cys831Arg-Ala832Gly-Gly833Val triple mutant. Mutants for which cleavage activity at the second site was higher than that of ΔMsc are marked with asterisks.

are unlikely candidates to correspond to the cleavage site. We examined the effects of deleting the 569-GlyAsp-570 and 982-AlaLys-983 dipeptides from ΔMsc on the processing of p90. In both cases, in vitro expression of ΔGD and ΔAK had no appreciable effect on the processing of the second-site cleavage products p90 and p70 (Fig. 3B). This is in contrast to the results obtained after the removal of the 832-AlaGly-833 dipeptide in ΔAG, which abolished p90 and p70 processing. The results of the radiosequence analysis of the labeled p90 cleavage product together with the deletion mutagenesis data indicate that the downstream cleavage site occurs between Ala832 and Gly833.

Characterization of the Ala832 ↓ Gly833 cleavage site. Processing at the Ala832 ↓ Gly833 cleavage site was examined for a group of ΔMsc mutants spanning the P5 to P2′ positions. The efficiency of cleavage of p90 for each mutant was determined by PhosphorImager analysis. The results of this analysis are shown on Fig. 4. Excluding the replacement of Cys831 by a glycine, most of the mutations at the P4, P3, P2, and P2′ positions were permissive for cleavage at the second site. The activities of the conservative mutants Phe829Tyr (P4), Cys831Ser (P2), and Lys834Arg (P2′) were 85% or higher than that of ΔMsc. Some nonconservative mutants also showed high levels of activity. Phe829Cys (P4), Pro830Ala (P3), Cys831Arg (P2), and Lys833Thr (P2′) each had a level of activity above 75%. Except for the conservative P1 substitution Ala832Gly (122%) and P5 substitution Arg828Lys (81%), the majority of the substitutions at the P5, P1, and P1′ positions severely reduced second-site proteolysis. Even for conservative changes, such as Ala832Val (P1) and Gly833Ala (P1′), the activity was reduced to between 31 and 34%.

The P2 residue of cellular papain-like proteinases plays an important role in the determination of cleavage specificity (22). Two P2 mutations, a conservative Cys831Ser and a nonconservative Cys831Arg, showed significant cleavage activity (>85%) at the second site, while a Cys831Gly mutant had only 21% of the activity of the ΔMsc standard (Fig. 4). The presence of an arginine at the P2 position also compensated for an inactivating mutation at P5. Although the activity of the Arg828Met mutant was 23%, further modification of this mutant with the replacement of Cys831 with an arginine increased the activity to 75%. The activity displayed by these two arginine mutants is noteworthy because the p28 cleavage site of MHV also has this amino acid at the P2 position (i.e., Arg246).

Exchange of the Gly247 ↓ Val248 and Ala832 ↓ Gly833 cleavage sites. We tested the ability of the PLP-1 to recognize the two cleavage sites at different positions by replacing each site for the other. First, we replaced the p28 site P1 and P1′ amino acids, glycine and valine, with those in the second site, alanine and glycine, respectively. These mutations were introduced into pSPNK, and their effects on the processing of p28 were measured by PhosphorImager analysis. The activity of the resulting double-mutant construct, pSPNK RGV→RAG, was 79% of that of pSPNK (Fig. 5A, lane 2). Thus, the PLP-1 has the ability to process the second-site scissile bond (i.e., Ala ↓ Gly) at the p28 cleavage site position. We previously studied the p28 processing activity of each of these mutations

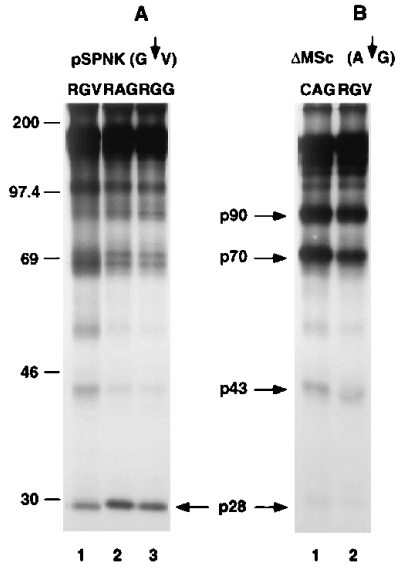

FIG. 5. Exchange of the cleavage sites recognized by the PLP-1. (A) Amino acid replacements at the p28 cleavage site in pSPNK. Plasmid DNA was in vitro transcribed and translated in TnT rabbit reticulocyte lysate in the presence of [^{35}S]methionine as described in Materials and Methods. Volumes of the radiolabeled lysates containing equivalent amounts of acid-precipitable counts were analyzed by SDS-PAGE (9% gel). Lane 1, pSPNK; lane 2, pSPNK RGV→RAG; lane 3, pSPNK RGV→RGG. The molecular masses of ^{14}C-labeled protein markers are indicated in kilodaltons to the left. The p28 cleavage in pSPNK occurs between Gly247 and Val248. The arrow indicates the migration of the cleavage product p28. (B) Amino acid replacements at the second cleavage site in ΔMsc. Plasmids ΔMsc (lane 1) and ΔMsc CAG→RGV (lane 2) were used for coupled in vitro transcription-translation. The arrows indicate the cleavage products p90, p70, p43, and p28. Coupled transcription-translation of pSPNK routinely generates an approximately 69-kDa polypeptide, observed across all lanes of panel A. This polypeptide is not a product of proteinase cleavage; it is a premature termination product, as evidenced by the fact that it synthesized in the presence of the cysteine proteinase inhibitor leupeptin (data not shown).

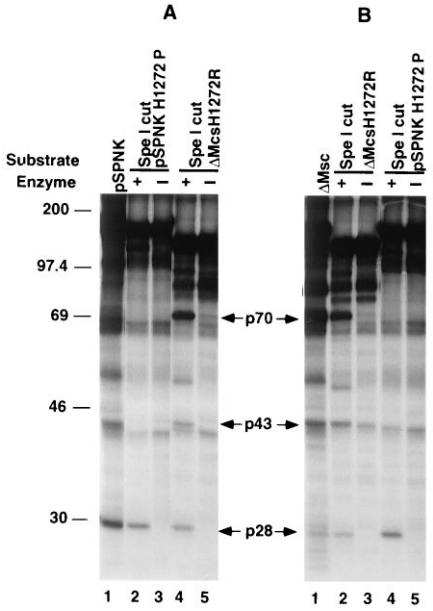

FIG. 6. Analysis of the *trans*-cleavage activity of the murine coronavirus PLP-1. PLP-1 enzyme was expressed from pSPNK or ΔMsc in the absence of radiolabeled amino acid unless otherwise noted. Unlabeled enzyme was then incubated with [^{35}S]methionine-labeled substrate and incubated at 20°C for 14 to 16 h. The + and − signs indicate the presence and absence of unlabeled enzyme in the posttranslational *trans*-cleavage assay. The molecular masses of ^{14}C-labeled protein markers are indicated in kilodaltons to the left of panel A. The cleavage products p70, p43, and p28 are indicated by arrows. (A) *trans* processing using pSPNK as the source of unlabeled enzyme. Lane 1, radiolabeled pSPNK control reaction; lane 2, pSPNK enzyme and pSPNK H1272R/*Spe*I-cut substrate; lane 3, pSPNK H1272P/*Spe*I-cut substrate; lane 4, pSPNK enzyme and ΔMsc H1272R/*Spe*I-cut substrate; lane 5, ΔMsc H1272R/*Spe*I-cut substrate. (B) *trans* processing using ΔMsc I as the source of unlabeled enzyme. Lane 1, radiolabeled ΔMsc I control reaction; lane 2, ΔMsc I enzyme and ΔMsc H1272R/*Spe*I-cut substrate; lane 3, ΔMsc H1272R/*Spe*I-cut substrate; lane 4, ΔMsc I enzyme and pSPNK H1272P/*Spe*I-cut substrate; lane 5, pSPNK H1272P/*Spe*I-cut substrate. The 69-kDa polypeptide generated from pSPNK is a premature termination product (see the legend to Fig. 5).

independently (20). The activity determined for the p28 cleavage site P1′ mutant pSPNK RGV→RGG was 86% (Fig. 5A, lane 3). Processing of p28 was less than 20% for the P1 mutant pSPNK RGV→RAV (data not shown). As noted before, the P1 amino acid at the p28 cleavage site (Gly247) plays a determinant role on the processing of p28 (14, 20). However, the detrimental effect of this substitution was compensated for by the simultaneous replacement of the P1′ Val248 with a glycine.

Cys831Arg, Ala832Gly, and Gly833Val mutations were simultaneously introduced into ΔMsc to replace the P2, P1, and P1′ amino acids at the second cleavage site with those found at the corresponding position of the p28 cleavage site. The p90 cleavage activity determined for the ΔMsc CAG→RGV triple mutant was 54% (Fig. 4B). Individually tested, both the Cys831Arg and Ala832Gly mutations showed an increase of about 20% in the level of proteolysis at the second site, while the Gly833Val replacement decreased the processing activity fivefold (Fig. 4). Although the PLP-1 was able to processes a second-site mutant resembling the p28 cleavage site, the presence of a glycine at the P1 position appears to be required for efficient processing.

***trans* processing by the PLP-1 at two sites.** The processing of p28 by the PLP-1 was suggested to occur only in *cis* (2). This observation was based on the absence of *trans* cleavage in an in vitro cotranslation assay using MHV-JHM genomic RNA as a source of enzyme and a synthetic RNA derived from the first 2 kb of ORF1a to generate substrate (2). Because the PLP-1 expressed from ΔMsc is capable of processing at two sites independently, we reexamined the ability of this proteinase to cleave in *trans* at these two sites by means of posttranslational *trans*-cleavage assays. Polypeptides containing an active PLP-1 domain were translated in the absence of a radioactive amino acid. Translations of pSPNK and ΔMsc served as the sources of enzyme. [^{35}S]methionine-labeled polypeptides containing the two target sites were used as substrates. To ensure the inability of the substrates to self-process, we selected plasmid templates containing a PLP-1-inactivating mutation of the catalytic His1272, H1272R (for ΔMsc), or H1272P (for pSPNK) (5). Furthermore, the templates were truncated at an *Spe*I restriction enzyme site between the two PLP-1 catalytic residues, thus removing the C-terminal portion of the PLP-1 domain. After independent expression of the PLP-1 and the substrates, reactions were stopped by the addition of DNase I, RNase A, and unlabeled methionine to the translation lysates. Subsequently, equal volumes of PLP-1 and substrate lysates were mixed together and analyzed under conditions similar to those used to test the *trans*-cleavage ability of the avian coronavirus 3C-like proteinase (33). Figures 6 and 7 show the results of the *trans*-cleavage assays. The proteolytic products from the *trans*-cleavage assay reactions were analyzed directly in the gels shown in Fig. 6. To verify their identities, the products were subsequently immunoprecipitated with polyclonal antiserum UP102, which recognizes p28, p43, and p70; this reduced background caused by prematurely terminated polypeptides with similar electrophoretic mobilities (Fig. 7). The p100 band, also observed in Fig. 7A, is the downstream product of cleavage of the truncated pSPNK substrate. PLP-1 enzyme synthesized either from pSPNK or ΔMsc and incubated in the presence of a

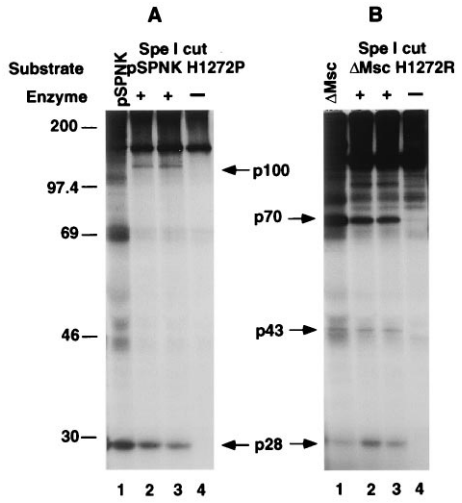

FIG. 7. Immunoprecipitation of *trans*-cleavage products of PLP-1. Polypeptide products generated in the in vitro *trans*-cleavage assay (Fig. 6) were immunoprecipitated with antiserum UP102 as described in Materials and Methods. The molecular masses of ^{14}C-labeled protein markers are indicated in kilodaltons to the left of panel A. The cleavage products p70, p43, p28, and p100 are indicated by arrows. (A) *trans* processing and UP102 immunoprecipitation of pSPNK substrates. Lane 1, radiolabeled pSPNK control reaction; lane 2, pSPNK enzyme and pSPNK H1272P/*Spe*I-cut substrate; lane 3, ΔMsc enzyme and pSPNK H1272P/*Spe*I-cut substrate; lane 4, radiolabeled pSPNK H1272P substrate linearized at the *Spe*I site. (B) *trans* processing and UP102 immunoprecipitation of ΔMsc substrate. Lane 1, radiolabeled ΔMsc control reaction; lane 2, ΔMsc enzyme and ΔMsc H1272R/*Spe*I-cut substrate; lane 3, pSPNK enzyme and ΔMsc H1272R/*Spe*I-cut substrate; lane 4, radiolabeled ΔMsc H1272R substrate linearized at the *Spe*I site. The 69-kDa polypeptide generated from pSPNK is a premature termination product (see the legend to Fig. 5).

ΔMsc-derived substrate produced the p28, p43, and p70 cleavage products derived from proteolysis at the 247-GlyVal-248 and 832-AlaGly-833 sites (Fig. 6A, lane 4; Fig. 6B, lane 2; Fig. 7B, lanes 2 and 3). However, substrates derived from the pSPNK template were processed only at the p28 site regardless of the origin of the PLP-1 proteinase (Fig. 6A, lane 2; Fig. 6B, lane 4; Fig. 7A, lanes 2 and 3). Two lines of evidence confirm that the presence of cleavage products did not result from *cis* processing. First, no cleavage products were observed from any incubation of substrate only (lanes 4 in Fig. 6A and B), indicating that the appearance of cleavage products was not the result of a substrate residual enzymatic activity or a proteolytic activity present in the reticulocyte lysates. Also, to corroborate the absence of protein synthesis during the coincubations of the unlabeled enzymes with the radiolabeled substrates, [^{35}S] methionine was added to a portion of each enzyme translation reaction after the addition of stop buffer. None of these control reactions generated detectable radiolabeled polypeptides (data not shown). Thus, the presence of cleavage products indicates the ability of the PLP-1 to process substrates in *trans*. These data also indicate that the difference in processing between pSPNK (i.e., one cleavage site) and ΔMsc (i.e., two cleavage sites) results from a differential access to the cleavage sites and not the nature of the proteinase.

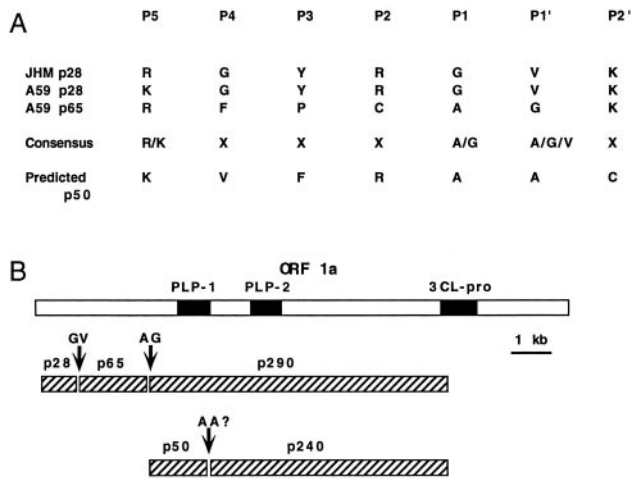

FIG. 8. Consensus sequence for PLP-1 cleavage and predicted in vivo cleavage sites in ORF 1a. (A) The sequences surrounding the p28 cleavage site for MHV-JHM and MHV-A59 are shown (14, 20). The sequence surrounding the second in vitro cleavage site is shown as the predicted p65 cleavage site for MHV-A59. A consensus sequence and a predicted p50 cleavage site as explained in Discussion are also shown. (B) A model for cleavages mediated within ORF1a by PLP-1 is shown along with the proteins detected in infected cells. The positions of PLP-1, the predicted second papain-like proteinase (PLP-2), and the 3C-like proteinase (3CL-pro) domains are shown as solid bars within ORF1a (open bar). ORF1a-encoded polypeptides are shown as cross-hatched bars. Cleavage sites believed to be mediated by PLP-1 are indicated with arrows. Based on electrophoretic mobility, p290 is predicted to extend into the 3CL-pro.

DISCUSSION

Viruses that infect eukaryotic hosts often require proteolytic processing by one or more types of proteinase activities to accomplish efficient genomic expression (15). In the case of the murine coronavirus, two distinct types of proteinases appear to be involved in the processing of its large nonstructural replicase polyprotein. The MHV PLP-1 belongs to the family of papain-like cysteine proteinases and is responsible for the in vitro cleavage of the amino-terminal product p28, a polypeptide that is also observed in MHV-infected cells (3, 5). This was the first activity identified for this proteinase. Previously we reported a second in vitro enzymatic activity for this proteinase in constructs bearing a partial deletion of the coding sequence between p28 and the proteinase domain. In this study, we have identified the location of this second cleavage to between the ORF1a amino acids Ala832 and Gly833. This conclusion is supported by the following observations. First, the in vitro translations of the deletion plasmids ΔMBst, ΔMsc.4, and ΔAG, all of which lack the 832-AlaGly-833 dipeptide, failed to generate polypeptides resulting from cleavage at this site. Second, most of the Ala832 and Gly833 mutations severely decreased proteolytic processing at the second cleavage site. This was in contrast to the effect of mutations of the adjacent amino acids, Cys831 and Lys834, most of which had near-wild-type levels of activity. In addition, the profile obtained after Edman degradation of the radiolabeled polypeptide (i.e., p90) downstream of the cleavage site was consistent with hydrolysis of the peptide bond between Ala832 and Gly833. Finally, the Ala832 ↓ Gly833 cleavage site resembles a typical viral papain-like cleavage site, which usually consists of amino acids with small uncharged side chains at the P1 and P1′ positions. For example, this new MHV cleavage site dipeptide is identical to that recognized by the nsP2 papain-like cysteine proteinase of several alphaviruses at the nsP1-nsP2 junction (32).

The role played by the P5 to P2′ amino acids surrounding the Ala832 ↓ Gly833 site on the processing at this site was studied in a series of site-directed mutants. The P5, P1, and P1′ positions were found to be more sensitive, even to conservative mutations, than the P4, P3, P2, and P2′ positions. With the exception of the Ala832Gly substitution at the P1 positions, all other P1 and P1′ mutants with larger or charged amino acid side chains decreased the processing activity to 32% or less. A majority (9 of 11) of the P4, P3, P2, and P2′ amino acid replacements retained substantial levels of activity. The cleavage activities of some of these mutants were enhanced (122 to 163%) relative to the parental ΔMsc plasmid. Included in this group were Phe829Tyr (P4), Cys831Arg (P2), Ala832Gly (P1), Lys834Thr (P2′), and Lys834Arg (P2′). Interestingly, three of these upregulating mutations confer a p28 cleavage site-like character to the second site. The Cys831Arg (P2) and Ala832Gly (P1) p28 mutants have the same amino acids as are present at the corresponding positions at the p28 cleavage site. The Phe829Tyr-enhanced cleavage mutant has a tyrosine at the P4 position, while the p28 cleavage site has a tyrosine at the P3 residue instead. The results suggest that mutations which increase the similarity of the Ala832 ↓ Gly833 cleavage site to the p28 site, with the exception of P1′ mutations, enhance cleavage at the second site.

Another notable observation was the activity of mutants with an arginine at the P2 position. The P2 amino acid plays a determinant role in the cleavage specificity of the related cysteine proteinases papain and cathepsin B (22). The plant proteinase papain shows a strong preference for substrates having an amino acid with a nonpolar bulky side chain (e.g., Phe and Tyr) at P2. The mammalian cathepsin B proteinase, on the other hand, has a broader specificity and can process substrates bearing either arginine or phenylalanine at the P2 position. We determined that the P2 mutation Cys831Arg upregulated processing at the second site. This mutation also compensated for the negative effect of an Arg828Met P5 mutation in a double mutant. An arginine is also present in the P2 position of the p28 cleavage site. These results may indicate that, at least in terms of substrate specificity, the PLP-1 could be described as a cathepsin B-like proteinase.

Three mutations were introduced simultaneously at the sec-

ond cleavage site of ΔMsc to create a p28-like cleavage site. The ΔMsc CAG→RGV triple mutant contains the p28 site P2, P1, and P1′ amino acids at the location of the second site. The P2 amino acid was also included in this mutant, given its determinant role on the proteolytic processing of p28 (14, 20). In a similar experiment, the P1 and P1′ amino acids at the p28 site were replaced by alanine and glycine, respectively, to reproduce the second cleavage site at that position (i.e., pSPNK RGV→RAG). The PLP-1 was able to process both of these cleavage site exchange mutants. The activity of the second-site triple mutant ΔMsc CAG→RGV (54%) appears to have been negatively determined by the substitution of the glycine with a valine at the P1′ position, as suggested by the low level of processing of the individual Gly833Val P1′ mutation in contrast with the individual Ala832Gly (P1) and Cys831Arg (P2) upregulating substitutions. Processing of the p28 site double mutant containing the second cleavage dipeptide was 86%. In this case, the role of the P1′ mutation was different. The negative effect that P1 mutations have on the processing of p28 was compensated for by the P1′ valine substitution with a glycine. It appears that the interaction of individual substrate residues with the proteinase is distinct for each cleavage site. The determinants of p28 cleavage site recognition by the PLP-1 have been analyzed for the A59 and JHM strains of MHV (14, 20). Although the number of second-site mutations that we examined was limited, a few comparisons can be established. In comparison to the p28 cleavage site, the Ala832 ↓ Gly833 cleavage shares in common the critical roles played by the P1 and P5 residues. With the notable exception of the second-site substitution Ala832Gly, which did not affect cleavage activity, all P1 mutations at both locations severely affected proteolytic processing. At the P5 position, only the conservative Arg828Lys mutation resulted in significant second cleavage site activity (81%). Another similarity between both sites is the flexibility of the PLP-1 to process most P4, P3, and P2′ mutations. The P2 residue plays significantly different roles at the two sites. The two studies cited above tested nine unique substitutions of the P2 residue (Arg246) at the p28 cleavage site, all of which resulted in a virtual elimination of p28 processing. This was true even for a conservative Arg246Lys replacement (20). On the other hand, the P2 residue (Cys831) of the cleavage site identified in this study was efficiently replaced both by a serine and an arginine. The importance of the P1′ amino acid also differs between the two sites. Production of p28 ranged from unaffected to dramatically reduced, depending on the amino acid replacement of valine at the P1′ residue of the p28 cleavage site. At the Ala832 ↓ Gly833 site, however, all three mutations tested reduced processing to 34% or less. It appears that only the amino acid with the smallest side chain (i.e., glycine) provides optimal processing at this site.

Our findings did not confirm that additional PLP-1 cleavage sites could potentially be identified by searching for the presence of Gly-Val dipeptides within the amino acid sequences encoded in gene 1 (14). The two sites recognized by the PLP-1 share the following similarities: a conserved basic amino acid at the P5 position that plays an important processing role and the cleavage between small neutral amino acids (Fig. 8). Therefore, we used a pattern consisting of a typical viral papain-like proteinase cleavage site flanked by a basic amino acid at the P5 position [P5-(R,K)XXX(G,A) ↓ (G,A,V)-P1′] to search the MHV-A59 replicase locus for potential cleavage sites. Only 10 sequences in ORF 1a and 8 sequences in ORF 1b matched this pattern. The ORF 1a sequence 1258-KVFRA ↓ A-1263 is the most interesting candidate among these. First, alanine dipeptides are cleaved by the nsP2 papain-like proteinase of alphaviruses (Table 2). This site also has similarities with the p28 cleavage site in that it has identical lysine and arginine residues at the putative P5 and P2 positions, respectively. Furthermore, the aromatic Phe1260 P3 residue resembles the P3 Tyr245 of p28 and the P4 Phe829 at the second site. Cleavage between Ala832 ↓ Gly833 and Ala1262 ↓ Ala1263 would generate a 47.4-kDa polypeptide which may correspond to the p50 cleavage product observed in MHV-A59-infected cells (12) and mapped to the same ORF1a region. *trans* processing at this proposed cleavage site, which is located between the catalytic dyad of the PLP-1, would inactivate the proteinase and thus could possibly provide a mechanism by which coronavirus polyprotein processing is regulated.

An unexpected finding of this study was the determination that the PLP-1 has the ability to act in *trans*. Baker and colleagues had previously characterized the murine coronavirus PLP-1 as an enzyme limited to *cis* processing (2). In that study, an in vitro-synthesized 65-kDa polypeptide which included p28 and downstream sequences failed to be processed in *trans* by the translation products of the MHV-JHM genome RNA. Equine arteritis virus, an arterivirus and member of the coronavirus-like superfamily, has a leader papain-like cysteine proteinase distantly related to coronavirus PLP-1 that was also reported to act only in *cis* near the amino terminus of its replicase locus (31). Our experiments, however, clearly demonstrate that the PLP-1 is able to process p28 in *trans* from substrates derived either from pSPNK or ΔMsc. *trans* processing at the Ala832 ↓ Gly833 site occurred from substrates derived from ΔMsc but not pSPNK, regardless of the origin of the PLP-1. This finding implies that the deletion in ΔMsc acts by making the second site more accessible to the PLP-1 rather than by altering the catalytic properties of the proteinase. The results shown in this study suggest that the MHV PLP-1 may be more like the alphavirus proteinase nsP2. The Sindbis virus nsP2 proteinase mediates the processing of the P1234 nonstructural polyprotein in a complex pathway that involves both *cis* and *trans* cleavages. The similarities between nsP2 and the PLP-1 (i.e., cleavage at more than one site and recognition of identical Ala ↓ Gly cleavage sites) suggest that the PLP-1 may play a more important role in the processing of the MHV replicase locus than previously thought.

Some important questions remain unresolved. First, why does the second cleavage site occur in ΔMsc and other constructs with deletions between the p28 and PLP-1 domains but not in the wild-type construct pSPNK? Our results indicate that the difference in processing is not due to a difference in the enzymes expressed from pSPNK and ΔMsc, since the PLP-1 equally processed different substrates in *trans* regardless of whether it was derived from pSPNK or ΔMsc. In addition to the p28 cleavage site encoded by ΔMsc, the 832-AlaGly-833 dipeptide is also accessible to the substrate binding pocket of the PLP-1 and efficiently processed. Assuming that the Ala832 ↓ Gly833 cleavage site is recognized in vivo, it is possible that the process involves a proteinase cofactor and/or that it occurs in a particular cellular location lacking in the in vitro translations of pSPNK. This factor appears not to be membranes since the addition of canine pancreatic membranes to the in vitro translations does not result in the production of p65 (data not shown). Second, does the Ala832 ↓ Gly833 cleavage site observed in cell-free translation systems correspond to the same cleavage site that generates the C terminus of p65 in vivo? The resemblance of the Ala832 ↓ Gly833 to other viral cysteine proteinase cleavage sites, in addition to the capacity of this site to generate a polypeptide similar in size to p65, strongly suggests that this may be the case.

We have recently cloned and overexpressed the PLP-1 domain in *Escherichia coli*. Now that we know that PLP-1 can

cleave in *trans*, we are planning to purify the *E. coli*-expressed protein to further study its enzymatic properties. We are also planning to carry out transfection experiments to verify whether the second cleavage site does indeed correspond to the C terminus of p65 and determine which factors are necessary for this second cleavage to occur.

ACKNOWLEDGMENTS

P.J.B. and S.A.H. contributed equally to this work.

We thank Xinhe Jiang for technical assistance, the Wistar Institute protein core facility, directed by David Speicher, for performing the protein microsequencing, and Alexander Gorbalenya for reading and making suggestions on the manuscript.

This work was supported by NIH grant AI-17418. P.J.B. and S.A.H. were partially supported by training grant NS-01780. P.J.B. was partially supported by an NIH research supplement for underrepresented minorities (NS-21954).

REFERENCES

1. **Agranovsky, A. A., E. V. Koonin, V. P. Boyko, E. Maiss, R. Frötschl, N. A. Lunina, and J. G. Atabekov.** 1994. Beet yellows closterovirus: complete genome structure and identification of a leader papain-like thiol protease. Virology **198:**311–324.
2. **Baker, S. C., C.-K. Shieh, L. H. Soe, M.-F. Chang, D. M. Vannier, and M. M. C. Lai.** 1989. Identification of a domain required for autoproteolytic cleavage of murine coronavirus gene A polyprotein. J. Virol. **63:**3693–3699.
3. **Baker, S. C., K. Yokomori, S. Dong, R. Carlisle, A. E. Gorbalenya, E. V. Koonin, and M. M. C. Lai.** 1993. Identification of the catalytic sites of a papain-like cysteine proteinase of murine coronavirus. J. Virol. **67:**6056–6063.
4. **Bonilla, P. J., A. E. Gorbalenya, and S. R. Weiss.** 1994. Mouse hepatitis virus strain A59 RNA polymerase ORF 1a: heterogeneity among MHV strains. Virology **198:**736–740.
5. **Bonilla, P. J., S. A. Hughes, J. D. Piñón, and S. R. Weiss.** 1995. Characterization of the leader papain-like proteinase of MHV-A59: identification of a new *in vitro* cleavage site. Virology **209:**489–497.
6. **Bransom, K. L., S. E. Wallace, and T. W. Dreher.** 1996. Identification of the cleavage site recognized by the turnip yellow mosaic virus protease. Virology **217:**404–406.
7. **Bredenbeek, P. J., C. J. Pachuck, A. F. H. Noten, J. Charité, W. Luytjes, S. R. Weiss, and W. J. M. Spaan.** 1990. The primary structure and expression of the second open reading frame of the polymerase gene of the coronavirus MHV-A59; a highly conserved polymerase is expressed by an efficient ribosomal frameshifting mechanism. Nucleic Acids Res. **18:**1825–1832.
8. **Carrington, J. C., S. M. Cary, T. D. Parks, and W. G. Dougherty.** 1989. A second proteinase encoded by a plant potyvirus genome. EMBO J. **8:**365–370.
9. **Chen, J.-P., J. H. Strauss, E. G. Strauss, and T. K. Frey.** 1996. Characterization of the rubella virus nonstructural protease domain and its cleavage site. J. Virol. **70:**4707–4713.
10. **Choi, G. H., R. Shapira, and D. L. Nuss.** 1991. Cotranslational autoproteolysis involved in gene expression from a double-stranded RNA genetic element associated with hypovirulence of the chestnut blight fungus. Proc. Natl. Acad. Sci. USA **88:**1167–1171.
11. **Denison, M. R., P. W. Zoltick, J. L. Leibowitz, C. J. Pachuk, and S. R. Weiss.** 1991. Identification of polypeptides encoded in open reading frame 1b of the putative polymerase gene of the murine coronavirus mouse hepatitis virus A59. J. Virol. **65:**3076–3082.
12. **Denison, M. R., P. W. Zoltick, S. A. Hughes, B. Giangreco, A. L. Olson, S. Perlman, J. L. Leibowitz, and S. R. Weiss.** 1992. Intracellular processing of the N-terminal ORF 1a proteins of the coronavirus MHV-A59 requires multiple proteolytic events. Virology **189:**274–284.
13. **Denison, M. R., S. A. Hughes, and S. R. Weiss.** 1995. Identification and characterization of a 65-kDa protein processed from the gene 1 polyprotein of the murine coronavirus MHV-A59. Virology **207:**316–320.
14. **Dong, S., and S. C. Baker.** 1994. Determinants of the p28 cleavage site recognized by the first papain-like cysteine proteinase of murine coronavirus. Virology **204:**541–549.
15. **Dougherty, W. G., and B. L. Semler.** 1993. Expression of virus-encoded proteinases: functional and structural similarities with cellular enzymes. Microbiol. Rev. **57:**781–822.
16. **Eleouet, J.-F., D. Rasschaert, P. Lambert, L. Levy, P. Vende, and H. Laude.** 1995. Complete sequence (20 kb) of the polyprotein-encoding gene 1 of transmissible gastroenteritis virus. Virology **206:**817–822.
17. **Gorbalenya, A. E., E. V. Koonin, A. P. Donchenko, and V. M. Blinov.** 1989. Coronavirus genome: prediction of putative functional domains in the nonstructural polyprotein by comparative amino acid sequence analysis. Nucleic Acids Res. **17:**4847–4861.
18. **Gorbalenya, A. E., E. V. Koonin, and M. M. C. Lai.** 1991. Putative papain-related thiol proteases of positive-strand RNA viruses. FEBS Lett. **288:**201–205.
19. **Herold, J., T. Raabe, B. Schelle-Prinz, and S. G. Siddell.** 1993. Nucleotide sequence of the human coronavirus 229E RNA polymerase locus. Virology **195:**680–691.
20. **Hughes, S. A., P. J. Bonilla, and S. R. Weiss.** 1995. Identification of the murine coronavirus p28 cleavage site. J. Virol. **69:**809–813.
21. **Kadaré, G., M. Rozanov, and A. L. Haenni.** 1995. Expression of the turnip yellow mosaic virus proteinase in Escherichia coli and determination of the cleavage site within the 206 kDa protein. J. Gen. Virol. **76:**2853–2857.
22. **Khouri, H. E., T. Vernet, R. Ménard, F. Parlati, P. Laflamme, D. C. Tessier, B. Gour-Salin, D. Y. Thomas, and A. C. Storer.** 1991. Engineering of papain: selective alteration of substrate specificity by site-directed mutagenesis. Biochemistry **30:**8929–8936.
23. **Kim, J. C., R. A. Spence, P. F. Currier, X. Lu, and M. R. Denison.** 1995. Coronavirus protein processing and RNA synthesis is inhibited by the cysteine proteinase inhibitor E64d. Virology **208:**1–8.
24. **Kirchweger, R., E. Ziegler, B. J. Lamphear, D. Waters, H.-D. Liebig, W. Sommergruber, F. Sobrino, C. Hohenadl, D. Blass, R. E. Rhoads, and T. Skern.** 1994. Foot-and-mouth disease virus leader proteinase: purification of the Lb form and determination of the cleavage site on eTF-4γ. J. Virol. **68:**5677–5684.
25. **Lawrence, D. M., M. N. Rozanov, and B. I. Hillman.** 1995. Autocatalytic processing of the 223-kDa protein of blueberry scorch carlavirus by a papain-like proteinase. Virology **207:**127–135.
26. **Lee, H.-J., C.-K. Shieh, A. E. Gorbalenya, E. V. Koonin, N. LaMonica, J. Tuler, A. Bagdzhadzhyan, and M. M. C. Lai.** 1991. The complete sequence (22 kilobases) of murine coronavirus gene 1 encoding the putative proteases and RNA polymerase. Virology **180:**567–582.
27. **Liu, D. X., I. Brierley, K. W. Tibbles, and T. D. K. Brown.** 1994. A 100-kilodalton polypeptide encoded by open reading frame (ORF) 1b of the coronavirus infectious bronchitis virus is processed by ORF 1a products. J. Virol. **68:**5772–5780.
28. **Liu, D. X., and T. D. K. Brown.** 1995. Characterisation and mutational analysis of an ORF 1a-encoding proteinase domain responsible for proteolytic processing of the infectious bronchitis virus 1a/1b polyprotein. Virology **209:**420–427.
29. **Lu, Y., X. Lu, and M. R. Denison.** 1995. Identification and characterization of a serine-like proteinase of the murine coronavirus MHV-A59. J. Virol. **69:**3554–3559.

29a. **Rozanov, M. N., L. A. Schiff, and S. R. Weiss.** Unpublished data.

30. **Shapira, R., and D. L. Nuss.** 1991. Gene expression by a hypovirulence-associated virus of the chestnut blight fungus involves two papain-like protease activities. J. Biol. Chem. **266:**19419–19425.
31. **Snijder, E. J., A. L. Wassenaar, and W. J. M. Spaan.** 1992. The 5′ end of the equine arteritis virus replicase gene encodes a papainlike cysteine protease. J. Virol. **66:**7040–7048.
32. **Strauss, J. H., and E. G. Strauss.** 1994. The alphaviruses: gene expression, replication, and evolution. Microbiol. Rev. **58:**491–562.
33. **Tibbles, K. W., I. Brierley, D. Cavanagh, and T. D. K. Brown.** 1996. Characterization in vitro of an autocatalytic processing activity associated with the predicted 3C-like proteinase domain of the coronavirus avian infectious bronchitis virus. J. Virol. **70:**1923–1930.
34. **Weiss, S. R., S. A. Hughes, P. J. Bonilla, J. D. Turner, J. L. Leibowitz, and M. R. Denison.** 1994. Coronavirus polyprotein processing. Arch. Virol. **9**(Suppl.)**:**349–358.
35. **Yoo, D., M. D. Parker, G. J. Cox, and L. A. Babiuk.** 1995. Zinc-binding of the cysteine-rich domain encoded in the open reading frame 1b of the RNA polymerase gene of coronavirus. Adv. Exp. Med. Biol. **380:**437–442.
36. **Ziebuhr, J., J. Herold, and S. G. Siddell.** 1995. Characterization of a human coronavirus (strain 229E) 3C-like proteinase activity. J. Virol. **69:**4331–4338.